*J. Fluid Mech.* (2022), *vol.* 931, R2, doi:10.1017/jfm.2021.936

JFM RAPIDS

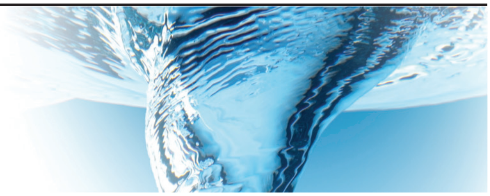

# Equilibrium tilt of slippery elliptical rods in creeping simple shear

**Darren G. Crowdy**†

Department of Mathematics, Imperial College London, 180 Queen's Gate, London SW7 2AZ, UK

(Received 6 September 2021; revised 19 October 2021; accepted 21 October 2021)

It is shown that shape anisotropy and intrinsic surface slip lead to equilibrium tilt of slippery particles in a creeping simple shear flow, even for nearly shape-isotropic particles with a cross-section that is close to circular provided the Navier-slip length is sufficiently large. We study a rigid particle with an elliptical cross-section, and of infinite extent in the vorticity direction, in simple shear. A Navier-slip boundary condition is imposed on its surface. When a Navier-slip length parameter $\lambda$ is infinite, an analytical solution is derived for the Stokes flow around a particle tilting in equilibrium at an angle $(1/2)\cos^{-1}((1-k)/(1+k))$ to the flow direction where $0 \leq k \leq 1$ is the ratio of the semi-minor to semi-major axes of its elliptical cross-section. A regular perturbation analysis about this analytical solution is then performed for small values of $1/\lambda$ and a numerical continuation method implemented for larger values. It is found that an equilibrium continues to exist for any anisotropic particle $k < 1$ provided $\lambda \geq \lambda_{crit}(k)$ where $\lambda_{crit}(k)$ is a critical Navier-slip length parameter determined here. As the case $k \to 1$ of a circular cross-section is approached, it is found that $\lambda_{crit}(k) \to \infty$, so the range of Navier-slip lengths allowing equilibrium tilt shrinks as shape anistropy is lost. Novel theoretical connections with equilibria for constant-pressure gas bubbles with surface tension are also pointed out.

**Key words:** particle/fluid flow

## 1. Introduction

In recent work Kamal, Gravelle & Botto (2020) have studied the motion of a thin rigid graphene nanoplatelet with hydrodynamic slip in a simple shear at low Reynolds numbers. They investigated the interesting observation that, at large Péclet numbers, interfacial slip suppresses an expected periodic rotation, resulting in the particle being in equilibrium with its principal axis tilted at a small angle with respect to the flow direction. Further studies of this equilibrium tilt of nanoplatelets have since been carried out including an exploration of finite Péclet number effects (Gravelle, Kamal & Botto 2021*a*,*b*). Earlier, Zhang, Xu &

† Email address for correspondence: d.crowdy@imperial.ac.uk

Qian (2015) explored the effect of surface slip on the so-called Jeffery orbits of rod-like particles of elliptical cross-section, although that investigation was limited to relatively small Navier-slip lengths and no equilibrium tilt was observed.

Kamal *et al.* (2020) remark that the observed tilt of the platelet is surprising in view of the classical work on ellipsoidal particles in shear by Jeffery (1922) who finds that a non-trivial rotation (the aforementioned Jeffery orbits) is generally expected to ensue when the particle boundary is a no-slip surface. Jeffery's work was extended by Bretherton (1962) who studied more general axisymmetric particle shapes and introduced an important determinant of the rotational dynamics known as the effective aspect ratio $k_{eff}$ which, it turns out, is relevant even when the particle surface admits slip. For no-slip particles with elliptical cross-section and of infinite extent in the vorticity direction $k_{eff} = k$ where $k$ is the ratio of the semi-minor to semi-major axes of the cross-section (Zhang *et al.* 2015; Kamal *et al.* 2020).

The observation of equilibrium tilt of slippery nanoplatelets is indeed surprising if one has in mind the work of Jeffery (1922) and Bretherton (1962). It is less surprising, however, in view of work on equilibria for constant-pressure gas bubbles in creeping slow viscous flows carried out shortly after Bretherton's work by Richardson (1968). Richardson addressed a significantly more challenging problem than that of Jeffery and Bretherton: the nonlinear free-boundary problem of determining the shape, if it exists, of a constant-pressure gas bubble, with surface tension active on its boundary, in equilibrium in an ambient simple shear. The non-dimensional parameter governing such a system is a capillary number, $Ca$ say, that measures the flow strength relative to that of surface tension. Remarkably, Richardson (1968) found analytical solutions to this free-boundary problem and unveiled the equilibrium bubble shapes to be elliptical with a $Ca$-dependent aspect ratio $k = k(Ca)$ and tilting at a $Ca$-dependent angle $\phi = \phi(Ca)$.

It need hardly be pointed out that gas bubbles and slippery particles are not the same, which is no doubt why bubbles are never mentioned in the slippery particle literature. The bubble problem is a two-phase fluid scenario while the notion of surface tension has no physical relevance for rigid particles. Consequently, the nature of the normal stress balance on the boundary of a rigid particle and a bubble are different. But consider a rigid particle in a fluid of viscosity $\mu$ with the Navier-slip condition (Luo & Pozrikidis 2008)

$$\frac{\lambda}{\mu}(t_i \sigma_{ij} n_j) = u_i t_i \tag{1.1}$$

on its boundary, where $\sigma_{ij}$ is the fluid stress tensor, $\lambda$ is the Navier-slip length parameter and $u_i$, $t_i$ and $n_i$ are, respectively, the fluid velocity, unit tangent and fluid-inward normal vector components at the boundary. In the limit $\lambda \to \infty$, this boundary condition becomes one of vanishing shear stress. That is, the same tangential stress condition as must pertain on the surface of a constant-pressure gas bubble. For equilibrium, both for a rigid particle or a bubble, one additionally requires that the boundary is a streamline of the flow. So far, then, the boundary conditions for the infinite-slip-length particle and constant-pressure gas bubble are the same. For a rigid particle, its shape is known and imposition of some far-field boundary condition then completes the problem statement. For the gas bubble, on the other hand, the equilibrium shape is unknown and, for given far-field flow conditions, has to be determined by further enforcement of a normal stress condition that any jump in normal fluid stress across the bubble boundary must be balanced by surface tension. The latter is what was done by Richardson (1968). Incidentally, it has since been shown that initially elliptical gas bubbles, including compressible ones where the bubble gas pressure obeys a given equation of state, remain elliptical under unsteady time evolution in a linear ambient Stokes flow with their shape parameters obeying a set of ordinary differential equations very much akin to the Jeffery equations relevant for evolving no-slip particles (Crowdy 2003).

An intriguing feature of Richardson's bubble solutions is that they exhibit an equilibrium tilt angle for all values of the capillary number which, moreover, cover all possible aspect ratios ranging from the shape-isotropic $k = 1$ case of a circular bubble to the $k = 0$ case of a finite-length shear-free slit. At the same time, the problem of a slippery rod-like particle with isotropic circular cross-section and with a Navier-slip condition (1.1) active on its boundary is so simple as to afford an explicit mathematical solution from which it is easy to deduce that the only solution for a torque-free circular particle equilibrium requires $\lambda = \infty$. In other words, there is no admissible equilibrium for a slippery circular rod if the Navier-slip length is finite (so that some frictional drag occurs at the surface). With this in mind, as well as Richardson's torque-free elliptical bubbles which also correspond to $\lambda = \infty$, one is inclined to the belief that there is no equilibrium tilt of slippery particles in a creeping simple shear unless they have an infinite Navier-slip parameter $\lambda$, that is, unless their boundaries are shear-free.

Yet the recent observations (Kamal *et al.* 2020) of equilibrium tilt for nanoplatelets are not consistent with that conclusion. Since nanoplatelets for which tilt has been observed are ostensibly long and thin (Kamal *et al.* 2020; Gravelle *et al.* 2021*a*,*b*) one suspects that significant shape anisotropy must play an important role in equilibrium tilt. Zhang *et al.* (2015) have explored the effect of shape anisotropy and Navier slip on the unsteady Jeffery orbits but they observed no tilting equilibria. Is it therefore only particles that are sufficiently long and thin that are amenable to equilibrium tilt? And is the tilt angle always small? Or is it possible that anisotropic particles of any aspect ratio can tilt in equilibrium provided the slip is sufficiently strong, as suggested by the constant-pressure bubble equilibria just discussed? It is clearly desirable to obtain a more complete picture of how all these facts fit together, and that is the purpose of the present paper.

Motivated by the similarities between slippery particles and gas bubbles just elucidated, we establish here that a rigid anisotropic rod-like particle of elliptical cross-section (i.e. $k < 1$) and with infinite Navier-slip length $\lambda$ also admits an equilibrium tilt angle $\phi$ which, since there is now no notion of a capillary number, we think of as a function of the particle aspect ratio, i.e. $\phi = \phi(k)$. For brevity, we call these 'elliptical particles'. Just as Richardson (1968) did for a gas bubble, we find an analytical solution to this slippery elliptical particle problem. It is important to note, however, that we cannot simply import Richardson's prior analysis because that relies critically on the normal stress jump on the boundary being balanced by surface tension, a feature simply not shared with the slippery particle problem where surface tension has no relevance. Richardson (1968) finds that the bubble equilibria turn out to have elliptical cross-section, that is, the same shape as our chosen class of rigid particles. We are therefore in a situation where we conjecture in advance that, in solving the slippery elliptical particle problem, we will retrieve Richardson's flow field around his bubble, but it must now be derived as the solution of a different boundary-value problem requiring a different solution scheme. Details of such a scheme are given here. For $\lambda = \infty$, it leads to an analytical solution to the slippery particle problem with equilibrium tilt angle $\phi$ related to the particle aspect ratio $k$ by

$$\phi = \phi_0(k) = \frac{1}{2}\cos^{-1}\left(\frac{1-k}{1+k}\right). \tag{1.2}$$

This relation is found to coincide with that obtained by eliminating the parametric dependence on $Ca$ between the expressions for $\phi(Ca)$ and $k(Ca)$ found for Richardson's elliptical bubble equilibria, as anticipated. For slippery particles the result (1.2), and its derivation, are new.

There are two benefits of having devised this new formulation of the infinitely-slippery particle problem. First, it can be used to find broad classes of analytical solutions for such particles having non-elliptical shape; those results will be presented elsewhere. Second, and the focus here, the formulation lends itself to a perturbation analysis in $1/\lambda \ll 1$ from which we obtain the explicit first-order correction to the tilt angle (1.2) as

$$\phi = \phi_0(k) - \frac{1}{2\lambda}\frac{B(\rho)}{A(\rho)} + O\left(\frac{1}{\lambda^2}\right), \quad \rho = \frac{1-k}{1+k}, \tag{1.3}$$

where

$$\left.\begin{aligned} A(\rho) &= 3\rho(1-\rho^2)\int_0^{2\pi} \frac{\sin(2\phi_0(k)) - \rho\sin(4\phi_0(k)+4\theta) + \sin(2\phi_0(k)+4\theta)}{(1+\rho^2-2\rho\cos(2\theta+2\phi_0(k)))^{5/2}}\,\mathrm{d}\theta, \\ B(\rho) &= -2\int_0^{2\pi} |Z_0'(\mathrm{e}^{\mathrm{i}\theta})|^2\left(\mathrm{Im}[I_0(\mathrm{e}^{\mathrm{i}\theta})] - \frac{1}{4}\right)\mathrm{d}\theta, \end{aligned}\right\} \tag{1.4}$$

and where explicit formulas for $I_0$ and $Z_0$ are given in (2.25) and (2.29). As discussed later, these formulas provide evidence that the range of possible slip lengths for equilibrium tilt shrinks as the isotropic case is approached. Then, for smaller $\lambda$, a numerical continuation scheme is also described that allows calculation of the rest of the equilibrium solution branch without difficulty. It is found that every anisotropic particle, even those close to circular, has a critical slip length, $\lambda_{crit}$, above which it will exhibit equilibrium tilt.

## 2. Mathematical formulation

It is convenient to use a complex variable formulation of two-dimensional Stokes flow. Such an approach has been used by the author to obtain the Jeffery-type differential equations governing the dynamics of no-slip curved rigid rods (Crowdy 2016) and we will adapt that analysis. Richardson (1968) also used complex analysis, but features of his scheme do not carry over to the rigid particle, as pointed out below. Using Re[·] and Im[·] to denote taking real and imaginary parts of a complex quantity, any steady incompressible Stokes flow $(u, v)$ in a two-dimensional $(x, y)$-plane can be described by a biharmonic streamfunction $\psi$ written as

$$\psi(z,\bar{z}) = \mathrm{Im}[\bar{z}f(z) + g(z)], \quad (u,v) = \left(\frac{\partial\psi}{\partial y}, -\frac{\partial\psi}{\partial x}\right), \quad u - \mathrm{i}v = 2\mathrm{i}\frac{\partial\psi}{\partial z}, \tag{2.1a–c}$$

where $f(z)$ and $g(z)$ are functions of $z = x + \mathrm{i}y$. From the Stokes equations it can be shown that the fluid pressure $P$, the vorticity $\omega = -\nabla^2\psi$ and the fluid rate-of-strain tensor $e_{ij} = (1/2)(\partial u_i/\partial x_j + \partial u_j/\partial x_i)$ are related to $f(z)$ and $g(z)$ by

$$4f'(z) = \frac{P}{\mu} - \mathrm{i}\omega, \quad u - \mathrm{i}v = -\overline{f(z)} + \bar{z}f'(z) + g'(z), \quad e_{11} + \mathrm{i}e_{12} = z\overline{f''(z)} + \overline{g''(z)}, \tag{2.2a–c}$$

where a prime symbol denotes a differentiation with respect to the argument of a function. The complexified expression for the boundary fluid stress $\sigma_{ij} = -Pn_i + 2\mu e_{ij}n_j$ is

$$-2\mu\mathrm{i}\frac{\mathrm{d}H}{\mathrm{d}s}, \quad H \equiv f(z) + z\overline{f'(z)} + \overline{g'(z)}, \tag{2.3}$$

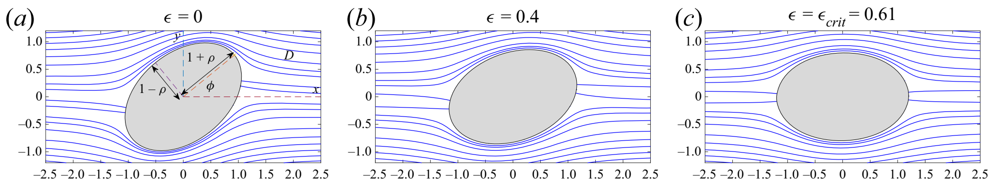


Figure 1. A slippery elliptical particle of aspect ratio $k = (1-\rho)/(1+\rho)$ with boundary condition (1.1) tilting at angle $\phi$ in simple shear with vorticity axis out of the plane. Streamlines, computed using the methods of this paper, for $\rho = 0.2$ for $\epsilon = (2\lambda)^{-1} = 0, 0.4$ and $0.61 (\approx \epsilon_{crit})$ are shown. The particle aligns with the flow as surface friction is added.

where $\mathrm{d}s = (\mathrm{d}z\,\overline{\mathrm{d}z})^{1/2}$ is the differential arclength element, with arclength $s$ increasing as the boundary is traversed with fluid to the left. A derivation of all the above fundamental relations is given in an appendix of Crowdy (2020). We want to find the relevant $f(z)$ and $g(z)$ for Stokes flow in the region $D$ shown in figure 1(*a*) exterior to a slippery elliptical particle centred at the origin. For a far-field simple shear flow with $(u, v) \to (y, 0)$, where we have set the flow time scale by picking the far-field shear rate to be unity, we need

$$f(z) \to \frac{\mathrm{i}}{4} z + O(1/z), \quad g(z) \to -\frac{\mathrm{i}}{4} z^2 + O(1), \quad \text{as } z \to \infty. \tag{2.4$a$,$b$}$$

In specifying (2.4*a*,*b*) the far-field fluid pressure is taken to vanish. The absence of any logarithmic singularities in the far-field behaviour (2.4*a*,*b*) of $f(z)$ and $g(z)$ guarantees that the particle will be free of any net force or torque, conditions necessary for equilibrium. An additive degree of freedom associated with the transformations $f(z) \mapsto f(z) + c$, $g'(z) \mapsto g'(z) + \bar{c}$ for any $c \in \mathbb{C}$ which leave invariant the expression for $u - \mathrm{i}v$ in (2.2*b*) has been set by insisting on the absence of a constant term in the far-field behaviour of $f(z)$.

The following conformal mapping transplants the unit disc $|\zeta| < 1$ in a parametric complex $\zeta$-plane to the unbounded fluid region $D$ exterior to the elliptical particle:

$$z = Z(\zeta) = \frac{a}{\zeta} + b\zeta, \quad a \in \mathbb{R}, \quad b = \rho\,\mathrm{e}^{2\mathrm{i}\phi}, \tag{2.5}$$

with $\zeta = 0$ corresponding to $z = \infty$. Let $\partial D$ denote the elliptical boundary. Writing $\zeta = \mathrm{e}^{\mathrm{i}\theta}$ it is easy to show that $|\zeta| = 1$ corresponds to the boundary of an ellipse with semi-major axis $a + \rho$ and semi-minor axis $a - \rho$ at angle $\phi$ to the positive real axis so its aspect ratio $k = (a-\rho)/(a+\rho)$; see figure 1. It is convenient to set the length scale by choosing $a = 1$ so that $\rho = (1-k)/(1+k)$. The particles will have different cross-sectional areas for different $\rho$ but any desired rescaling of the equilibria can be done *a posteriori*. The Schwarz function $S(z)$ of the boundary $\partial D$ is the function, analytic in an annular neighbourhood of $\partial D$, satisfying $\bar{z} = S(z)$ when $z \in \partial D$. Since $|\zeta| = 1$ on $\partial D$,

$$S(z) = \overline{Z(\zeta)} = a\zeta + \frac{\bar{b}}{\zeta}, \quad \text{for } z \in \partial D, \text{ or for } |\zeta| = 1. \tag{2.6}$$

Substituting for $1/\zeta$ from (2.5) tells us $S(z)$ is analytic in $D$ except at infinity where

$$S(z) = \bar{b}\left(\frac{Z(\zeta)}{a} - \frac{b\zeta}{a}\right) + a\zeta = \frac{\bar{b}}{a} Z(\zeta) + \zeta\left(a - \frac{|b|^2}{a}\right) \to \frac{\bar{b}}{a} z + O(1/z), \quad \text{as } z \to \infty. \tag{2.7}$$

Now let

$$g(z) = -S(z) f(z) + \hat{g}(z). \tag{2.8}$$

The appearance of $\hat{g}(z)$ here differs from the bubble analysis of Richardson (1968) who took the bubble pressure (and not the far-field pressure) to vanish and used the normal stress balance to argue that $\hat{g}(z) = 0$. The rigid particle problem does not afford us this luxury. But, fortunately, $\hat{g}(z)$ is easy to determine. On $\partial D$,

$$\psi = \mathrm{Im}[\bar{z}f(z) + g(z)] = \mathrm{Im}[\bar{z}f(z) - S(z)f(z) + \hat{g}(z)] = \mathrm{Im}[\hat{g}(z)] = 0, \tag{2.9}$$

since $\partial D$ must be a streamline, $\psi$ vanishing on $\partial D$ without loss of generality. As $z \to \infty$,

$$g(z) = -S(z)f(z) + \hat{g}(z) \to -\frac{\mathrm{i}}{4}\frac{\bar{b}}{a}z^2 + O(1) + \hat{g}(z), \tag{2.10}$$

implying, in order that $g(z)$ satisfies (2.4*b*),

$$\hat{g}(z) \to \frac{\mathrm{i}}{4}\left(\frac{\bar{b}}{a} - 1\right)z^2 + O(1), \quad z \to \infty. \tag{2.11}$$

Since $\hat{g}(z)$ is otherwise analytic in the fluid then, as a function of $\zeta$, we deduce that

$$\hat{g}(z) = \frac{Ca^2}{\zeta^2} + \bar{C}a^2\zeta^2 := G(\zeta), \quad C = \frac{\mathrm{i}}{4}\left(\frac{\bar{b}}{a} - 1\right). \tag{2.12}$$

This satisfies both (2.9) and (2.11). Equation (2.8) implies that, at the boundary $\partial D$,

$$H = \mathrm{i}\gamma z_s + \overline{\hat{g}'(z)}, \quad u + \mathrm{i}v = -\Gamma z_s + \overline{\hat{g}'(z)}, \quad \gamma = 2\,\mathrm{Im}\left[\frac{f(z)}{z_s}\right] \quad \Gamma = 2\,\mathrm{Re}\left[\frac{f(z)}{z_s}\right], \tag{2.13$a$–$d$}$$

where we use the shorthand $z_s = \mathrm{d}z/\mathrm{d}s$ for the complexified unit tangent and we have used the fact that $\mathrm{d}S/\mathrm{d}z = \overline{z_s}/z_s$ for $z \in \partial D$. Equations (2.3) and (2.13*a*) imply

$$-2\mu\mathrm{i}\frac{\mathrm{d}H}{\mathrm{d}s} = 2\mu\left(\frac{\mathrm{d}\gamma}{\mathrm{d}s}z_s + \gamma z_{ss}\right) - 2\mu\mathrm{i}\overline{\hat{g}''(z)}\overline{z_s}, \quad \text{where } z_{ss} = \frac{\mathrm{d}^2z}{\mathrm{d}s^2}. \tag{2.14}$$

On use of the streamline condition (2.9), as well as (2.3) and (2.14), we find

$$\left.\begin{aligned}\frac{\lambda}{\mu}(t_i\sigma_{ij}n_j) &= \frac{\lambda}{\mu}\mathrm{Re}\left[\overline{z_s}\left(-2\mu\mathrm{i}\frac{\mathrm{d}H}{\mathrm{d}s}\right)\right] = 2\lambda\left(\frac{\mathrm{d}\gamma}{\mathrm{d}s} + \mathrm{Im}\left[\hat{g}'(z)z_{ss}\right]\right),\\ t_iu_i &= \mathrm{Re}[\overline{z_s}(-\Gamma z_s + \overline{\hat{g}'(z)})] = -\Gamma + \mathrm{Re}[\hat{g}'(z)z_s].\end{aligned}\right\} \tag{2.15}$$

The Navier-slip condition (1.1) on the particle surface can therefore be written as

$$\frac{\mathrm{d}\gamma}{\mathrm{d}s} = -\mathrm{Im}[\hat{g}'(z)z_{ss}] + \epsilon(-\Gamma + \mathrm{Re}[\hat{g}'(z)z_s]), \quad \epsilon = \frac{1}{2\lambda}. \tag{2.16}$$

On integration with respect to $s$, this becomes

$$\gamma = \int_0^s \{-\mathrm{Im}[\hat{g}'(z)z_{\tilde{s}\tilde{s}}] + \epsilon(-\Gamma + \mathrm{Re}[\hat{g}'(z)z_{\tilde{s}}])\}\,\mathrm{d}\tilde{s} + \sigma, \tag{2.17}$$

where $\sigma$ is a real constant. It follows from the chain rule that

$$\frac{\mathrm{d}z}{\mathrm{d}s} = \frac{\mathrm{i}\zeta Z'(\zeta)}{|Z'(\zeta)|}, \quad \frac{\mathrm{d}^2z}{\mathrm{d}s^2} = -\frac{\zeta Z'(\zeta)}{|Z'(\zeta)|^2}\left(1 + \mathrm{Re}\left[\frac{\zeta Z''(\zeta)}{Z'(\zeta)}\right]\right). \tag{2.18$a$,$b$}$$

Putting these facts together (2.17) can be stated, at a boundary point $\zeta = \mathrm{e}^{\mathrm{i}\theta}$, as

$$\tilde{\gamma}(\zeta) = R(\zeta) + \sigma, \quad \text{with } \tilde{\gamma}(\zeta) \equiv -2|Z'(\zeta)| \mathrm{Re}\left[\frac{f(Z(\zeta))}{\zeta Z'(\zeta)}\right], \tag{2.19}$$

$$R(\zeta) = \int_0^\theta \left\{ \mathrm{Im}[\eta G'(\eta)] \left( \frac{1}{|Z'(\eta)|} \left( 1 + \mathrm{Re}\left[\frac{\eta Z''(\eta)}{Z'(\eta)}\right]\right) - \epsilon \right) - \epsilon \tilde{\Gamma}(\eta)|Z'(\eta)| \right\} \mathrm{d}\phi, \quad \eta = \mathrm{e}^{\mathrm{i}\phi},$$
$$\text{with } \tilde{\Gamma}(\zeta) \equiv 2|Z'(\zeta)| \mathrm{Im}\left[\frac{f(Z(\zeta))}{\zeta Z'(\zeta)}\right]. \tag{2.20}$$

For $f(z)$ to be single-valued we need $R(\zeta)$ to be single-valued around $|\zeta| = 1$, or

$$\int_0^{2\pi} \left\{ \mathrm{Im}[\zeta G'(\zeta)] \left( \frac{1}{|Z'(\zeta)|} \left( 1 + \mathrm{Re}\left[\frac{\zeta Z''(\zeta)}{Z'(\zeta)}\right]\right) - \epsilon \right) - \epsilon \tilde{\Gamma}(\zeta)|Z'(\zeta)| \right\} \mathrm{d}\theta = 0. \tag{2.21}$$

This solvability condition ensures the particle is free of net force and torque.

### 2.1. *Analytical solution for $\epsilon = 0$*

When $\epsilon = 0$, the dependence of $R(\zeta)$ on $f(z)$ disappears and (2.19) becomes

$$\mathrm{Re}\left[\frac{f(Z(\zeta))}{\zeta Z'(\zeta)}\right] = -\frac{1}{2|Z'(\zeta)|}\left(R_0(\zeta) + \sigma\right), \quad \text{for } \zeta = \mathrm{e}^{\mathrm{i}\theta}, \tag{2.22}$$

where

$$R_0(\zeta) = \int_0^\theta \left\{ \mathrm{Im}[\eta G'(\eta)] \left( \frac{1}{|Z'(\eta)|} \left( 1 + \mathrm{Re}\left[\frac{\eta Z''(\eta)}{Z'(\eta)}\right]\right)\right)\right\} \mathrm{d}\phi, \quad \eta = \mathrm{e}^{\mathrm{i}\phi}. \tag{2.23}$$

Since, for univalency, $Z'(\zeta) \neq 0$ inside the unit $\zeta$ disc, and since $\zeta Z'(\zeta) \to -(a/\zeta) \to -z$ as $z \to \infty$ or $\zeta \to 0$, it follows from the far-field requirement (2.4*a*) on $f(z)$ that the function whose real part is taken in (2.22) is an analytic function of $\zeta$ inside the unit disc. Supposing $\sigma$ known, (2.22) becomes a classical Schwarz problem in the unit disc for the analytic function in square brackets in (2.22). The Poisson integral formula gives

$$f(z) = f(Z(\zeta)) = \zeta Z'(\zeta)(I_0(\zeta) + \mathrm{i}\, d), \quad d \in \mathbb{R}, \tag{2.24}$$

where

$$I_0(\zeta) = -\frac{1}{2\pi \mathrm{i}} \oint_{|\eta|=1} \frac{\mathrm{d}\eta}{\eta} \frac{\eta + \zeta}{\eta - \zeta} \left( \frac{R_0(\eta) + \sigma}{2|Z'(\eta)|} \right). \tag{2.25}$$

To satisfy the far-field condition (2.4*a*) on $f(z)$, we must pick $d = -1/4$ and arrange that $I_0(0) = I_0'(0) = 0$. Now $I_0(0) = 0$ provided that the heretofore unspecified $\sigma$ is chosen as

$$\sigma = -\left( \oint_{|\zeta|=1} \frac{\mathrm{d}\zeta}{\zeta} \frac{R_0(\zeta)}{|Z'(\zeta)|} \right) \Big/ \left( \oint_{|\zeta|=1} \frac{\mathrm{d}\zeta}{\zeta} \frac{1}{|Z'(\zeta)|} \right). \tag{2.26}$$

This leaves no freedoms to enforce the requirement $I_0'(0) = 0$. But $Z(-\zeta) = -Z(\zeta)$ and we expect, on the grounds of the symmetry of the geometrical arrangement and the background shear, that $f(-z) = -f(z)$. This means, from (2.24), that $I_0(-\zeta) = I_0(\zeta)$ and, consequently, that $I_0'(-\zeta) = -I_0'(\zeta)$ allowing us to infer that $I_0'(0) = 0$ automatically. All requirements are then satisfied and the solution is fully determined provided only that the solvability condition (2.21) with $\epsilon = 0$ can be satisfied: it is this that decides the equilibrium tilt angle $\phi$. On use of (2.12), with $\epsilon = 0$, some algebra reduces (2.21) to

$$\int_0^{2\pi} \frac{\rho\cos(2\theta+2\phi) - \cos 2\theta}{(1+\rho^2 - 2\rho\cos(2\theta+2\phi))^{3/2}}\,\mathrm{d}\theta = 0. \tag{2.27}$$

This crucial equilibrium condition can be satisfied by noticing that on setting $\rho = \cos 2\phi$ a trigonometric addition formula turns the integrand's numerator into $-\sin 2\phi \sin(2\theta + 2\phi)$, rendering the integrand an exact differential of a $2\pi$-periodic function whose integral is then zero, as required. Thus $\rho = \cos 2\phi$ provides solvability and the tilt angle is given by (1.2). The corresponding $f(z)$ is given by (2.24) with $d = -1/4$ and $I_0(\zeta)$ and $\sigma$ specified in (2.25) and (2.26), respectively; $g(z)$ is then given by (2.8) and (2.12).

Kamal *et al.* (2020) discuss the nanoplatelet dynamics in terms of Bretherton's effective aspect ratio parameter, which they call $k_e$, where $\mathrm{d}\phi/\mathrm{d}t \propto k_e^2\cos^2\phi + \sin^2\phi$. Equilibrium requires $\mathrm{d}\phi/\mathrm{d}t = 0$ hence, on use of double-angle formulas, $\cos 2\phi = (1+k_e^2)/(1-k_e^2)$ which, on comparison with (1.2), shows that our results for infinitely slippery elliptical particles ($\lambda = \infty$) would correspond to a pure imaginary $k_e = \mathrm{i}\sqrt{k}$.

### 2.2. *First-order correction to equilibrium tilt angle for* $0 < \epsilon \ll 1$

For $\epsilon \ll 1$, we expect a regular perturbation,

$$f(z) = f_0(z) + \epsilon f_1(z) + \cdots, \quad \hat{g}(z) = \hat{g}_0(z) + \epsilon\hat{g}_1(z) + \cdots \quad \phi = \phi_0 + \epsilon\phi_1 + \cdots, \tag{2.28$a$–$c$}$$

where we rename the $f(z)$, $\hat{g}(z)$ and $\phi$ just found explicitly for $\epsilon = 0$ as $f_0(z)$, $\hat{g}_0(z)$ and $\phi_0$ and set $b = \rho\,\mathrm{e}^{2\mathrm{i}\phi_0}$. For modified tilt, the conformal mapping and Schwarz function require $O(\epsilon)$ corrections:

$$\left.\begin{aligned} Z(\zeta) = \frac{a}{\zeta} + b\zeta + 2\mathrm{i}\epsilon\phi_1 b\zeta = Z_0(\zeta) + \epsilon Z_1(\zeta), \quad Z_0(\zeta) \equiv \frac{a}{\zeta} + b\zeta, \quad Z_1(\zeta) \equiv 2\mathrm{i}\phi_1 b\zeta, \\ S(z) = S_0(z) - \frac{2\mathrm{i}\epsilon\bar{b}\phi_1}{\zeta}, \quad S_0(z) = a\zeta + \frac{\bar{b}}{\zeta}. \end{aligned}\right\} \tag{2.29}$$

We are only interested here in determining $\phi_1$: this will emerge on substituting (2.28*a*–*c*) into the solvability condition (2.21). It turns out only $\hat{g}_1(z)$ is needed for this, and that is easy to find. For $f(z)$ to have the same far-field behaviour as $f_0(z)$, we insist that $f_1(z)$ is $O(1/z)$ as $z \to \infty$ then with $g(z) = -S(z)f(z) + \hat{g}(z)$ as in (2.8), on substitution of (2.28*a*–*c*) and use of the streamline condition on the boundary, it can be shown that, to within an unimportant constant,

$$\hat{g}_1(z) = \frac{Ea^2}{\zeta^2} + \bar{E}a^2\zeta^2, \quad E = \frac{\bar{b}\phi_1}{2a}. \tag{2.30}$$

On expanding (2.21) for small $\epsilon$, the equation emerging at $O(\epsilon)$, after considerable algebra and using (2.30), is found to be $A(\rho)\phi_1 + B(\rho) = 0$ which gives (1.3) and (1.4).

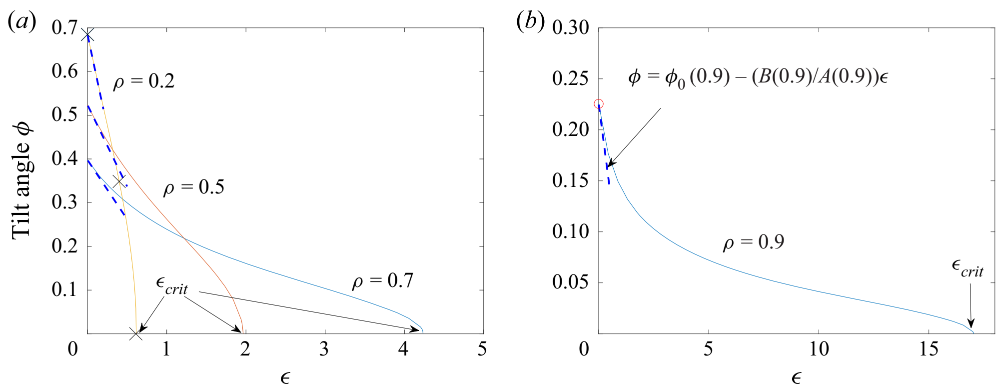


Figure 2. Equilibrium tilt angle $\phi$ as a function of $\epsilon$. A branch of equilibria emanates from the ordinate axis at $\phi_0 = (1/2)\cos^{-1}(\rho)$ for every $0 < \rho < 1$; the cases shown are (*a*) $\rho = 0.2, 0.5, 0.7$ and (*b*) $\rho = 0.9$. The tangent lines $\phi - \phi_0 = -(A(\rho)/B(\rho))\epsilon$ from the perturbation analysis at $\epsilon = 0$ are shown (dashed): as $\rho \to 0$ their gradient tends to $-\infty$. Each solution branch hits $\phi = 0$ (alignment with the shear) at $\epsilon = \epsilon_{crit}$.

### 2.3. *Numerical scheme for arbitrary* $\epsilon$

The above formulation leads naturally to an iterative numerical scheme for arbitrary $\epsilon > 0$. We can make an initial guess for $\phi$ and for the complex coefficients $\{F_n | n \geq 1\}$ in

$$f(z) = \frac{\mathrm{i}a}{4\zeta} + \sum_{n\geq 1} F_n \zeta^n. \tag{2.31}$$

The solvability condition (2.21), together with the expressions (2.20), (2.26) and

$$f(z) = \zeta Z'(\zeta)\left(I(\zeta) - \frac{\mathrm{i}}{4}\right), \quad I(\zeta) = -\frac{1}{2\pi\mathrm{i}}\oint_{|\eta|=1} \frac{\eta+\zeta}{\eta-\zeta}\left(\frac{R(\eta)+\sigma}{2|Z'(\eta)|}\right)\frac{\mathrm{d}\eta}{\eta}, \tag{2.32}$$

then provide iterative updates on these initial guesses as part of a numerical continuation scheme (Newton's method) from $\epsilon = 0$. The analytical solution for $\epsilon = 0$ makes a natural choice of initial guess, but taking $\phi = \phi_0 = (1/2)\cos^{-1}\rho$ and initializing all the coefficients $\{F_n | n \geq 1\}$ to be zero is also found to lead to ready convergence to solutions over the range $0 < \rho \leq 0.9$ that have been calculated here.

Figure 2(*a*) shows the tilt angle $\phi$ as a function of $\epsilon$ for $\rho = 0.2, 0.5$ and 0.7. Crosses on the $\rho = 0.2$ curve are solutions whose streamlines are shown in figure 1. Interestingly, a non-trivial branch is found for each choice of aspect ratio $k < 1$, or equivalently, for any anisotropic particle with $\rho = (1-k)/(1+k) > 0$. The tangent lines at $\epsilon = 0$ computed using (1.3)–(1.4) are also shown providing a consistency check on both the perturbation analysis and the numerical algorithm. Each equilibrium branch is found to hit the $\epsilon$ axis, where the major particle axis aligns with the background shear, at a critical value $\epsilon_{crit}$ defining a critical value $\lambda_{crit} = (2\epsilon_{crit})^{-1}$ of the Navier-slip length below which we conjecture that an equilibrium no longer exists. The branch for $\rho = 0.9$, where the particle has length 3.8 and thickness 0.2 and closely resembles a thin nanoplatelet, is shown separately in figure 2(*b*) because it exists for such a large range of $\epsilon$; we find $\epsilon_{crit} \approx 17$. It follows that $\lambda_{crit} = (2\epsilon_{crit})^{-1} \approx 1/34$ which is smaller than the particle thickness so slip lengths of the order of its thickness will exhibit equilibrium tilt. This is consistent with the observations of Kamal *et al.* (2020) for nanoplatelets. Figure 3(*a*) shows $\lambda_{crit}$, renormalized with respect to an effective radius $\sqrt{1-\rho^2}$ so that all particle cross-sectional

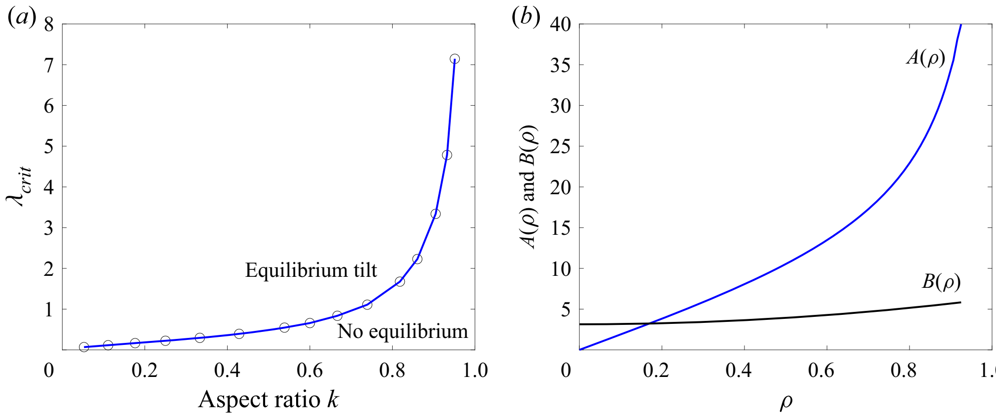


Figure 3. (*a*) Critical slip length $\lambda_{crit} = (2\epsilon_{crit})^{-1}$ non-dimensionalized with respect to an effective radius for which all particles have cross-sectional area π. Close-to-circular anisotropic particles ($k \to 1$ or $\rho \to 0$) tilt at close to 45° but only exist for Navier-slip parameters large compared with their effective radius. (*b*) $A(\rho)$ and $B(\rho)$ as functions of $\rho$.

areas are π, as a function of $k = (1-\rho)/(1+\rho)$. For near-circular particles, or $k$ approaching 1, $\lambda_{crit}$ is seen to be significantly larger than the effective radius which is close to unity. Indeed figure 2(*a*) shows that, as $\rho \to 0$ ($k \to 1$), $\epsilon_{crit}$ decreases and the solution branches tend to infinite negative slope as $\rho \to 0$. The explicit formulas (1.4) reveal that $A(\rho)$ vanishes as $\rho \to 0$ while $B(\rho)$ tends to a non-zero constant – see figure 3(*b*) – confirming this infinite negative gradient at $\rho = 0$ for a shape-isotropic circular particle. This indicates the range of slip parameters for equilibrium tilt vanishes as $\rho \to 0$, i.e. $\epsilon_{crit} \to 0$, $\lambda_{crit} \to \infty$, which is consistent with the aforementioned fact that analysis of a circular rod reveals torque-free equilibrium only for $\lambda = \infty$ ($\epsilon = 0$).

Our results furnish a more complete picture of how particle shape anisotropy works in tandem with intrinsic surface slip to produce equilibrium tilt. The phenomenon is not restricted to thin platelets: we have shown there is a delicate balance between shape anisotropy and surface slip most readily observed for thin particles (because the values of $\lambda_{crit}$ are lower) but not exclusive to them. We have focused on elliptical particles but our work suggests that any particle that is not shape isotropic will have an intrinsic critical Navier-slip parameter in creeping simple shear. Incidentally, weak inertial effects at small but finite Reynolds numbers are also known to halt the expected Jeffery-type rotational dynamics in favour of equilibrium tilt (Subramanian & Koch 2005). The results here imply a different alternative mechanism: intrinsic surface slip. The dynamical interplay between these two distinct physical effects is clearly of significant interest.

Another ramification of our work is that, since the solution to the rigid elliptical particle problem with $\lambda = \infty$ has been shown to coincide with the capillary gas-bubble problem, we can infer that the normal stress balance on the elliptical particle is effectively one given by a fictional surface tension: that is, the normal stress on the rigid particle is a linear function of the surface curvature (a fixed linear function for a given particle, but a different linear function for different particles). On most of a long thin particle this normal stress will be nearly constant, getting larger only near the particle edges where the curvature gets large. For $\lambda$ large but finite, it is reasonable to expect the normal stress will be close, within $O(1/\lambda)$, to that given by this 'effective surface tension'. Previous authors (Singh *et al.* 2014; Gravelle *et al.* 2021*a*) have studied similar edge effects for thin particles but without this novel theoretical connection to surface tension in view.

It has been more common when studying slip to take the no-slip case $\lambda = 0$ (Jeffery 1922; Bretherton 1962) as the theoretical baseline and to gradually add slip. This paper has made the case that it can be more enlightening to start in the no-shear-stress scenario, or infinite Navier-slip length $\lambda = \infty$, and to gradually add friction.

**Declaration of interests.** The author reports no conflict of interest.

**Author ORCIDs.**
Darren G. Crowdy https://orcid.org/0000-0002-7162-0181.

## References

BRETHERTON, F.P. 1962 The motion of rigid particles in a shear flow at low Reynolds number. *J. Fluid Mech.* **14**, 284–304.

CROWDY, D.G. 2003 Compressible bubbles in Stokes flow. *J. Fluid Mech.* **476**, 345–356.

CROWDY, D.G. 2016 Flipping and scooping of curved 2D rigid fibers in simple shear: the Jeffery equations. *Phys. Fluids* **28**, 053105.

CROWDY, D.G. 2020 Collective viscous propulsion of a two-dimensional flotilla of Marangoni boats. *Phys. Rev. Fluids* **5**, 124004.

GRAVELLE, S., KAMAL, C. & BOTTO, L. 2021*a* Alignment of a flexible platelike particle in shear flow: effect of surface slip and edges. *Phys. Rev. Fluids* **6**, 084102.

GRAVELLE, S., KAMAL, C. & BOTTO, L. 2021*b* Violations of Jeffery's theory in the dynamics of nanographene in shear flow. *Phys. Rev. Fluids* **6**, 034303.

JEFFERY, G.B. 1922 The motion of ellipsoidal particles immersed in a viscous fluid. *Proc. R. Soc.* A **102**, 161–179.

KAMAL, C., GRAVELLE, S. & BOTTO, L. 2020 Hydrodynamic slip can align thin nanoplatelets in shear flow. *Nat. Commun.* **11**, 2425.

LUO, H. & POZRIKIDIS, C. 2008 Effect of surface slip on Stokes flow past a spherical particle in infinite fluid and near a plane wall. *J. Engng Maths* **62**, 1–21.

RICHARDSON, S. 1968 Two-dimensional bubbles in slow viscous flows. *J. Fluid Mech.* **33**, 476–493.

SINGH, V., KOCH, D.L., SUBRAMANIAN, G. & STROOCK, A.D. 2014 Rotational motion of a thin axisymmetric disk in a low Reynolds number linear flow. *Phys. Fluids* **26**, 033303.

SUBRAMANIAN, G. & KOCH, D.L. 2005 Inertial effects on fibre motion in simple shear flow. *J. Fluid Mech.* **535**, 383–414.

ZHANG, J., XU, X. & QIAN, T. 2015 Anisotropic particle in viscous shear flow: Navier slip, reciprocal symmetry, and Jeffery orbit. *Phys. Rev.* E **91**, 033016.